ARTICLE

doi:10.1038/nature11820

Hastatic order in the heavy-fermion compound URu_2Si_2

Premala Chandra[1], Piers Coleman[1,2] & Rebecca Flint[3]

The development of collective long-range order by means of phase transitions occurs by the spontaneous breaking of fundamental symmetries. Magnetism is a consequence of broken time-reversal symmetry, whereas superfluidity results from broken gauge invariance. The broken symmetry that develops below 17.5 kelvin in the heavy-fermion compound URu_2Si_2 has long eluded such identification. Here we show that the recent observation of Ising quasiparticles in URu_2Si_2 results from a spinor order parameter that breaks double time-reversal symmetry, mixing states of integer and half-integer spin. Such 'hastatic' order hybridizes uranium-atom conduction electrons with Ising $5f^2$ states to produce Ising quasiparticles; it accounts for the large entropy of condensation and the magnetic anomaly observed in torque magnetometry. Hastatic order predicts a tiny transverse moment in the conduction-electron 'sea', a colossal Ising anisotropy in the nonlinear susceptibility anomaly and a resonant, energy-dependent nematicity in the tunnelling density of states.

The hidden order that develops below $T_{HO} = 17.5$ K in the heavy-fermion compound URu_2Si_2 is particularly notable, having eluded identification for 25 years[1–12]. Recent spectroscopic[13–17], magnetometric[18] and high-field measurements[19,20] suggest that the hidden order is connected with the formation of an itinerant heavy-electron fluid, as a consequence of quasiparticle hybridization between localized, spin–orbit-coupled *f*-shell moments and mobile conduction electrons. Although the development of hybridization at low temperatures is usually associated with a crossover, in URu_2Si_2 both optical[17] and tunnelling[14–16] probes suggest that it develops abruptly at the hidden-order transition, leading to proposals[9,10] that the hybridization is an order parameter.

Ising quasiparticles

High-temperature bulk susceptibility measurements on URu_2Si_2 show that the local $5f$ moments embedded in the conduction-electron sea are Ising in nature[1,21], and quantum oscillation experiments deep within the hidden-order phase[22] reveal that the quasiparticles possess a giant Ising anisotropy[20,23,24]. The Zeeman splitting $\Delta E(\theta)$ depends solely on the *c*-axis component of the magnetic field: $\Delta E = g(\theta)\mu_B B$ (ref. 24). Here B is the magnetic field, μ_B is the Bohr magneton and the empirically determined *g*-factor takes the form $g(\theta) = g\cos(\theta)$, where θ is the angle between the magnetic field and the *c* axis and g is the Ising *g*-factor. The *g*-factor anisotropy exceeds 30, corresponding to an anisotropy of the Pauli susceptibility in excess of 900; this anisotropy is also observed in the angle dependence of the Pauli-limited upper critical field of the superconducting state[23,24], showing that the Ising quasiparticles pair to form a heavy-fermion superconductor. This giant anisotropy suggests that the f moment is transferred to the mobile quasiparticles through hybridization[25].

In the tetragonal crystalline environment of URu_2Si_2, such Ising anisotropy is most natural in an integer-spin $5f^2$ configuration of the uranium ions[4,26]. Although a variety of singlet crystal-field schemes have been proposed[6,27], the observation of paired Ising quasiparticles in a superconductor with a transition temperature of $T_c \approx 1.5$ K indicates that this $5f^2$ configuration is doubly degenerate to within an energy resolution of $g\mu_B H_{c2} \approx 5$ K, where H_{c2} is the upper critical field of the superconductor. Moreover, the observation of multiple spin zeroes in the quantum oscillations, resulting from the interference of Zeeman split orbits in a tilted field, requires that in a transverse field the underlying $5f^2$ configuration is doubly degenerate to within a cyclotron energy, which is $\hbar\omega_c = \hbar eB/m^* \approx 1.5$ K for the largest extremal orbit[20,22] (α) ($m^* = 12.5m_e$ measured in $B = 13.9$ T, where m_e is the electron mass). These tiny bounds suggest that the Ising $5f^2$ state is intrinsically degenerate. In URu_2Si_2, tetragonal symmetry protects such a magnetic non-Kramers Γ_5 doublet[28], the candidate origin of the Ising quasiparticles[4,29].

The quasiparticle hybridization of half-integer-spin conduction electrons with an integer-spin doublet in URu_2Si_2 has profound implications for hidden order; such mixing can not occur without the breaking of double time-reversal symmetry. Time-reversal, $\hat{\Theta}$, is an anti-unitary quantum operator with no associated quantum number[30]. However double time-reversal, $\hat{\Theta}^2$, which is equivalent to a 2π rotation, forms a unitary operator with an associated quantum number, the 'Kramers index', K (ref. 30). For a quantum state of total angular momentum J, $K = (-1)^{2J}$ defines the phase factor acquired by its wavefunction after two successive time-reversals: $\hat{\Theta}^2|\psi\rangle = K|\psi\rangle = |\psi^{2\pi}\rangle$. An integer-spin state $|\alpha\rangle$ is unchanged by a 2π rotation, and so $|\alpha^{2\pi}\rangle = +|\alpha\rangle$ and $K = 1$. However, conduction electrons with half-integer-spin states, $|k\sigma\rangle$, where k is the vector momentum and σ is the spin component, change sign: $|k\sigma^{2\pi}\rangle = -|k\sigma\rangle$. Hence, $K = -1$ for conduction electrons.

Double time-reversal symmetry

Although conventional magnetism breaks time-reversal symmetry, it is invariant under $\hat{\Theta}^2$, with the result that the Kramers index is conserved. However, in URu_2Si_2 the hybridization between integer-spin and half-integer-spin states requires a quasiparticle mixing term of the form $\mathcal{H} = |k\sigma\rangle V_{\sigma\alpha}(k)\langle\alpha| + \text{H.c.}$, where H.c. indicates Hermitian

[1]Center for Materials Theory, Department of Physics and Astronomy, Rutgers University, 136 Frelinghuysen Road, Piscataway, New Jersey 08854-8019, USA. [2]Department of Physics, Royal Holloway, University of London, Egham, Surrey TW20 0EX, UK. [3]Department of Physics, Massachusetts Institute for Technology, Massachusetts Avenue, Cambridge, Massachusetts 02139-4307, USA.

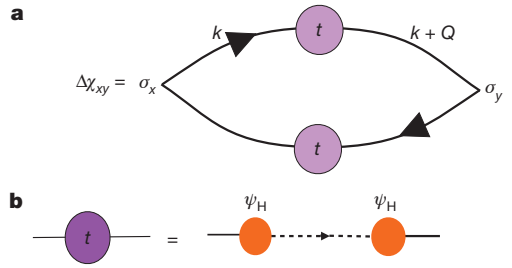

Figure 1 | Phenomenological interpretation of the anomalous spin susceptibility in URu_2Si_2. **a**, The anomalous spin susceptibility is given by conduction electrons (solid lines) scattering off the hidden-order parameter, sandwiched between σ_x and σ_y vertices. **b**, The anomalous scattering t matrix can be rewritten as a resonant scattering off the order parameter. The dashed lines represent f electrons and the ψ_H vertex represents scattering off the hidden-order parameter.

conjugate, in the low-energy fixed-point Hamiltonian. After two successive time-reversals

$$|k\sigma\rangle V_{\sigma\alpha}(k)\langle\alpha| \rightarrow |k\sigma^{2\pi}\rangle V^{2\pi}_{\sigma\alpha}(k)\langle\alpha^{2\pi}| = -|k\sigma\rangle V^{2\pi}_{\sigma\alpha}(k)\langle\alpha|$$

Because the microscopic Hamiltonian is time-reversal invariant, it follows that $V_{\sigma\alpha}(k) = -V^{2\pi}_{\sigma\alpha}(k)$; the hybridization thus breaks time-reversal symmetry in a fundamentally new way, forming an order parameter that, like a spinor, reverses under 2π rotations. The resulting 'hastatic' order (*hasta* is Latin for spear), is a state of matter that breaks both single and double time-reversal symmetry and is thus distinct from conventional magnetism.

Indirect support for time-reversal symmetry breaking in the hidden-order phase is provided by recent magnetometry measurements that indicate the development of an anisotropic basal-plane spin susceptibility, χ_{xy}, at the hidden-order transition[18]. The strong Ising anisotropy of the f electrons prevents them from responding in the basal plane, which leads us to interpret χ_{xy} as a anomalous conduction electron response (Fig. 1), induced by scattering off the hidden-order parameter. In this interpretation, the associated scattering matrix must mix the x and y components of the conduction electron spins and must take the form $t(k) = (\sigma_x \pm \sigma_y)d(k)$, where $d(k)$ is the scattering amplitude. The scattering matrix $t(k)$ has recently been linked to a spin nematic state[11], under the special condition that $d(-k) = -d^*(k)$ (where an asterisk denotes complex conjugation) to avoid time-reversal symmetry breaking. However, in our interpretation, $d(k)$ is associated with resonant scattering off the Ising f state, a process with a real, even-parity scattering amplitude, $d(k) = d(-k)$. In this case, the observed t matrix is necessarily odd under time-reversal in the hidden-order phase.

Hybridization in heavy-fermion compounds is usually driven by valence fluctuations mixing a ground-state Kramers doublet and an excited singlet (Fig. 2a). In this case, the hybridization amplitude is a scalar that develops via a crossover, leading to mobile heavy fermions. However, valence fluctuations from a $5f^2$ ground state create excited states with an odd number of electrons and, hence, a Kramers degeneracy (Fig. 2b). Then the quasiparticle hybridization has two components, Ψ_σ, that determine the mixing of the excited Kramers doublet into the ground state. These two amplitudes form a spinor defining the hastatic-order parameter

$$\Psi = \begin{pmatrix} \Psi_\uparrow \\ \Psi_\downarrow \end{pmatrix}$$

The presence of distinct up and down hybridization components indicates that Ψ carries the global spin quantum number; the onset of hybridization must now break double time-reversal and spin rotational invariance by means of a phase transition.

Under pressure, URu_2Si_2 undergoes a first-order phase transition from the hidden-order state to an antiferromagnetic (AFM) state[31]. These two states are remarkably close in energy and share many key features[19,32,33] including common Fermi surface pockets; this motivated the recent proposal that despite the first-order transition separating the two phases, they are linked by 'adiabatic continuity'[32], corresponding to a notional rotation of the hidden order in internal parameter space[5,34]. In the magnetic phase, this spinor points along the c axis

$$\Psi_A \propto \begin{pmatrix} 1 \\ 0 \end{pmatrix}$$

$$\Psi_B \propto \begin{pmatrix} 0 \\ 1 \end{pmatrix}$$

corresponding to time-reversed configurations on alternating layers A and B, implying a large staggered Ising moment. For the hidden-order state, the spinor points in the basal plane

$$\Psi_A \approx \frac{1}{\sqrt{2}} \begin{pmatrix} e^{-i\phi/2} \\ e^{i\phi/2} \end{pmatrix}$$

$$\Psi_B \approx \frac{1}{\sqrt{2}} \begin{pmatrix} -e^{-i\phi/2} \\ e^{i\phi/2} \end{pmatrix}$$

where, again, $\Psi_B = \Theta\Psi_A$, and the hidden order is protected from developing a large moment by the pure Ising character of the $5f^2$ ground state.

Hastatic order permits a direct realization of the adiabatic continuity between the hidden-order and AFM phases in terms of a single Landau functional for the free energy

$$f[T,P,B_z] = \left[\alpha(T_{HO} - T) - \eta_z B_z^2\right]|\Psi|^2 + \beta|\Psi|^4 - \gamma\left(\Psi^\dagger\sigma_z\Psi\right)^2$$

where $\gamma = \delta(P - P_c)$ (δ being the Dirac delta function) is a pressure-tuned anisotropy term and a dagger denotes adjoint. The unique feature of the theory is that the non-Kramers doublet has Ising

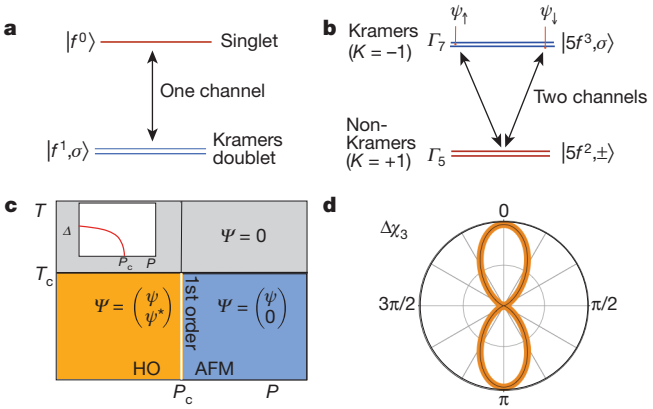

Figure 2 | Spinor hybridization and signatures of hastatic order. **a**, A normal Kondo effect occurs in ions with an odd number of f electrons, where the ground state is guaranteed to be doubly degenerate by time-reversal symmetry (and is known as a Kramers doublet). Virtual valence fluctuations to an excited singlet state are associated with a scalar hybridization. **b**, In URu_2Si_2, quasiparticles inherit an Ising symmetry from a $5f^2$ non-Kramers doublet. Loss or gain of an electron necessarily leads to an excited Kramers doublet, and the development of a coherent hybridization is associated with a two-component spinor hybridization that carries a magnetic quantum number and must therefore develop at a phase transition. **c**, Phase diagram for hastatic order, showing how tuning the parameter $\lambda \propto P - P_c$ leads to a spin flop between hastatic order and Ising magnetic order. Inset: at the first-order line, the longitudinal spin gap, Δ, is predicted to vanish because $\Delta \propto \sqrt{P_c - P}$. **d**, Polar plot showing the predicted $\cos^4(\theta)$ form of the nonlinear susceptibility, χ_3, induced by hastatic order, where θ is the angle between the magnetic field and the c axis.

character and couples only to the z component of the magnetic field, $B_z = B\cos(\theta)$. The resulting Ising splitting of the non-Kramers doublet suppresses the Kondo effect, giving rise to the B_z^2 term in the quadratic coefficient, where the coefficient η_z is of order $1/T_{\rm HO}^2$ (Supplementary Information). The phase diagram predicted by this free energy is shown in Fig. 2c. When $P < P_c(T)$, the vector $\Psi^\dagger\vec{\sigma}\Psi = |\Psi|^2(n_x,n_y,0)$ (where $\vec{\sigma} = (\sigma_1,\sigma_2,\sigma_3)$) denotes a vector of the three Pauli matrices) lies in the basal plane, resulting in hastatic order. At $P = P_c$, there is a first-order 'spin flop' into a magnetic state where $\Psi^\dagger\vec{\sigma}\Psi = |\Psi|^2(0,0,\pm 1)$ lies along the c axis.

Adiabatic continuity provides a natural interpretation of the soft, or low-energy, longitudinal spin fluctuations observed to develop in the hidden-order state[35] as an incipient Goldstone excitation between the two phases[34]. In the hidden-order state, rotations between hastatic and AFM order will lead to a gapped Ising collective mode that we identify with the longitudinal spin fluctuations observed in inelastic neutron scattering[35]. At the first-order phase transition, where $P = P_c$, the quartic anisotropy term vanishes; we predict that the gap, Δ, to longitudinal spin fluctuations will soften according to $\Delta \propto \sqrt{\gamma|\Psi|^2} \approx |\Psi|\sqrt{P_c(T) - P}$ (Supplementary Information). Experimental observation of this feature would provide confirmation of the common origin of the hidden and AFM order.

Another prediction of the phenomenological theory is the development of a nonlinear susceptibility anomaly with a colossal Ising anisotropy. From the Landau theory (Supplementary Information), the jump in the specific heat, ΔC, the susceptibility anomaly, $\mathrm{d}\chi_1/\mathrm{d}T$, and the nonlinear susceptibility anomaly, $\Delta\chi_3$, obey the relation $(\Delta C/T_{\rm HO})\Delta\chi_3 = 12(\mathrm{d}\chi_1/\mathrm{d}T)^2$, where $\mathrm{d}\chi_1/\mathrm{d}T = -(\alpha/2\beta)\eta_z\cos^2(\theta)$, such that $\Delta\chi_3 \propto \cos^4(\theta)$ (Fig. 2d). A large anomaly in the c-axis nonlinear susceptibility of URu_2Si_2 has been observed at $T_{\rm HO}$ (refs 21, 36), but its Ising anisotropy has never been quantified. The development of a colossal Ising anisotropy in the zero-field nonlinear susceptibility at the hidden-order transition is predicted to be another consequence of hastatic order.

Two-channel valence fluctuation model

We now present a model that relates hastatic order to the valence fluctuations in URu_2Si_2 and is based on a two-channel Anderson lattice model. The uranium ground state is a $5f^2$ Ising Γ_5 doublet[4], $|\pm\rangle = a|\pm 3\rangle + b|\mp 1\rangle$, written in terms of $J = 5/2$ f electrons in the three tetragonal orbitals $\Gamma_7^\pm$ and Γ_6:

$$|+\rangle = \left(af^\dagger_{\Gamma_7^-\downarrow}f^\dagger_{\Gamma_7^+\downarrow} + bf^\dagger_{\Gamma_6\uparrow}f^\dagger_{\Gamma_7^+\uparrow}\right)|0\rangle$$
$$|-\rangle = \left(af^\dagger_{\Gamma_7^-\uparrow}f^\dagger_{\Gamma_7^+\uparrow} + bf^\dagger_{\Gamma_6\downarrow}f^\dagger_{\Gamma_7^+\downarrow}\right)|0\rangle$$

The lowest-lying excited state is most likely the $5f^3$ ($J = 9/2$) state, but for simplicity here we take it to be the symmetry-equivalent $5f^1$ state. Valence fluctuations from the ground state ($5f^2$ Γ_5) to the excited state ($5f^1$ $\Gamma_7^\pm$) occur in two orthogonal conduction channels[37,38], Γ_7^- and Γ_6. This allows us to read off the hybridization matrix elements of the Anderson model

$$H_{\rm VF}(j) = V_6 c^\dagger_{\Gamma_6\pm}(j)\left|\Gamma_7^+\pm\right\rangle\langle\Gamma_5\pm| + V_7 c^\dagger_{\Gamma_7\mp}(j)\left|\Gamma_7^+\mp\right\rangle\langle\Gamma_5\pm| + \mathrm{H.c.}$$

where the plus and minus signs respectively denote the 'up' and 'down' states of the coupled Kramers and non-Kramers doublets. The field $c^\dagger_{\Gamma\sigma}(j) = \sum_k \left[\Phi^\dagger_\Gamma(k)\right]_{\sigma\tau} c^\dagger_{k\tau}e^{-ik\cdot R_j}$ creates a conduction electron at site j (at position R_j) with spin σ in a Wannier orbital with symmetry $\Gamma \in \{\Gamma_6,\Gamma_7\}$, and V_6 and V_7 are the corresponding hybridization strengths. The full model is then written

$$H = \sum_{k\sigma}\epsilon_k c^\dagger_{k\sigma}c_{k\sigma} + \sum_j\left[H_{\rm VF}(j) + H_{\rm a}(j)\right]$$

where $H_{\rm a}(j) = \Delta E\sum_\pm \left|\Gamma_7^+\pm,j\right\rangle\left\langle\Gamma_7^+\pm,j\right|$ is the atomic Hamiltonian.

Hastatic order is revealed by factorizing the Hubbard operators, $\left|\Gamma_7^+\sigma\right\rangle\langle\Gamma_5\alpha| = \hat{\Psi}^\dagger_\sigma\chi_\alpha$. Here $|\Gamma_5\alpha\rangle = \chi^\dagger_\alpha|\Omega\rangle$ is the non-Kramers doublet, represented by the pseudo-fermion $\chi^\dagger_\alpha$, and $\hat{\Psi}^\dagger_\sigma$ is a slave boson[39] representing the excited f^1 doublet $\left|\Gamma_7^+\sigma\right\rangle = \hat{\Psi}^\dagger_\sigma|\Omega\rangle$. Hastatic order is the condensation of this boson, $\Psi^\dagger_\sigma\chi_\alpha \to \left\langle\hat{\Psi}_\sigma\right\rangle\chi_\alpha$, generating a hybridization between the conduction electrons and the Ising $5f^2$ state while also breaking double time-reversal symmetry. The Γ_5 doublet has both magnetic and quadrupolar moments represented by $\chi^\dagger\vec{\sigma}\chi = \left(\mathcal{O}_{x^2-y^2},\mathcal{O}_{xy},m^z\right)$, where m^z is the Ising magnetic moment and $\mathcal{O}_{x^2-y^2}$ and $\mathcal{O}_{xy}$ are quadrupole moments. The tensor product $Q_{\alpha\beta} \equiv \Psi_\alpha\Psi^\dagger_\beta$ describes the development of composite order between the non-Kramers doublet and the spin density of conduction electrons. Composite order has been considered previously by several authors in the context of two-channel Kondo lattices[37,40,41] in which the valence fluctuations have been integrated out. However, by factorizing the composite order in terms of the spinor Ψ_α, we are able to understand directly the development of coherent Ising quasiparticles and the broken double time-reversal symmetry.

Using this factorization, we can rewrite the valence fluctuation term as

$$H_{\rm VF}(j) = \sum_k c^\dagger_{k\sigma}\hat{\mathcal{V}}_{\sigma\eta}(k,j)\chi_\eta(j)e^{-ik\cdot R_j} + \mathrm{H.c.}$$

where $\hat{\mathcal{V}}(k,j) = V_6\Phi^\dagger_{\Gamma_6}(k)\hat{B}^\dagger_j + V_7\Phi^\dagger_{\Gamma_7^-}(k)\hat{B}^\dagger_j\sigma_1$ with

$$\hat{B}_j = \begin{pmatrix}\hat{\Psi}_\uparrow & 0\\ 0 & \hat{\Psi}_\downarrow\end{pmatrix}$$

In the ordered state, $B_j = \left\langle\hat{B}_j\right\rangle$ is replaced by its expectation value, such that in the hidden-order state

$$\left\langle B^\dagger_j\right\rangle = |\Psi|\begin{pmatrix}e^{i(Q\cdot R_j+\phi)/2} & 0\\ 0 & e^{-i(Q\cdot R_j+\phi)/2}\end{pmatrix} \equiv |\Psi|U_j$$

with magnitude $|\Psi|$. The internal angle, ϕ, rotates B_j within the basal plane.

Because the hidden-order and AFM phases seem to share a single commensurate wavevector, $Q = (0,0,2\pi/c)$ (refs 19, 32, 33), we use this wavevector here. It is convenient to absorb the unitary matrix U_j into the pseudo-fermion, such that $\tilde{\chi}_j = U_j\chi_j$. This gauge transformation transfers the charge from the slave boson to the pseudo-fermion, making it a charged quasiparticle. In this gauge, one channel (Γ_6) is uniform whereas the other (Γ_7^-) is staggered, and the valence fluctuation Hamiltonian becomes

$$H_{\rm VF} = \sum_k c^\dagger_k\mathcal{V}_6(k)\chi_k + c^\dagger_k\mathcal{V}_7(k)\chi_{k+Q} + \mathrm{H.c.}$$

where the hybridization form factors are $\mathcal{V}_7(k) = V_7\Phi^\dagger_7(k)\sigma_1$ and $\mathcal{V}_6(k) = V_6\Phi^\dagger_6(k)$

g-factor anisotropy

There are two general aspects of this condensation that deserve special comment. First, the two-channel Anderson impurity model is known to possess a non-Fermi liquid ground state with an entanglement entropy of $(1/2)k_B\ln(2)$ (ref. 42). The development of hastatic order in the lattice liberates this zero-point entropy, accounting naturally for the large entropy of condensation. As a slave boson, Ψ carries both the charge, e, of the electrons and the local gauge charge, $Q_j = \Psi^\dagger_j\Psi_j + \chi^\dagger_j\chi_j$, of constrained valence fluctuations, and its condensation gives a mass to their relative phase through the Higg's

mechanism[43]. But as a Schwinger boson, Ψ's condensation breaks the SU(2) spin symmetry. In this way the hastatic boson can be regarded as a magnetic analogue of the Higg's boson.

One of the key elements of the hastatic theory is the formation of mobile Ising quasiparticles, and the observed Ising anisotropy enables us to set some of the parameters of the theory. The full anisotropic g-factor is a combination of f-electron and conduction-electron components given by $g(\theta) \approx g\cos\theta + g_c\left(\frac{T_K}{D}\right)$ where $g = 2.6$, $g_c = 2$ and the factor T_K/D (T_K, Kondo temperature; D, conduction-electron bandwidth) derives from the small conduction-electron admixture in the quasiparticles. Experimentally[20], the g-factor anisotropy, that is, the ratio of the c-axis and basal-plane g-factors, $g_z/g_\perp \approx D/T_K$, is in excess of 30, which enables us phenomenologically to set a lower bound on D/T_K in our model. The g-factor is defined in terms of the Zeeman splitting of the heavy-fermion dispersion, $\Delta E_{k\eta} = |E_{k\eta\uparrow} - E_{k\eta\downarrow}| = g_{k\eta}(\theta)\mu_B B$, where $\eta \in [1,4]$ is a band index. Figure 3a shows the Fermi-surface-averaged g-factor, defined by

$$\bar{g}(\theta) = \frac{\sum_{k\eta} g_{k\eta}(\theta)\delta(E_{k\eta})}{\sum_{k\eta}\delta(E_{k\eta})}$$

and calculated within the mean-field hastatic model, as a function of field angle to the c axis, choosing the lower-bound estimate $D/T_K \approx 30$.

Broken time–reversal and nematicity

Another key aspect of the hastatic picture is that there must be time-reversal symmetry breaking in both the hidden-order and the AFM phases, manifested by a staggered moment; in the AFM phase this leads to a large c-axis f-electron moment, but in the hidden-order phase it becomes a small transverse moment carried by conduction electrons, $\vec{m}_c = -g\mu_B \mathrm{Tr}\vec{\sigma}\mathcal{G}^c(k,k+Q)$, where $\mathcal{G}^c$ is the conduction-electron Green's function (Supplementary Information). The small magnitude of the induced moment is a consequence of the Clogston–Anderson compensation theorem, which states that changes in the conduction-electron magnetization are set by the same ratio, T_K/D, that determines the g-factor anisotropy[44]. There will also be a small mixed-valent contribution from the excited Kramers doublet, $\vec{m}_1 \propto \langle \Psi^\dagger \vec{\sigma} \Psi \rangle$. The angle of the moments in the plane is controlled by the internal hastatic angle, ϕ. Figure 3b shows the temperature dependence of the in-plane magnetic moment, $m_\perp$, calculated for a case where $D/T_K \approx 30$, for which $m_\perp(0) = 0.015\mu_B$, an upper bound for the predicted conduction-electron moment. Neutron scattering measurements on URu_2Si_2 have placed bounds on the c-axis magnetization of the f electrons using a momentum transfer, Q, in the basal plane. Detection of an $m_\perp(0)$ carried by conduction electrons, with a small scattering form-factor, will require high-resolution measurements with a c-axis momentum transfer. We note that there have been reports from muon spin relaxation and NMR measurements[45,46] of very small intrinsic basal-plane fields in URu_2Si_2, which are consistent with this theory.

Although the conduction electrons develop a magnetic moment, in the hastatic-ordered state, the non-Kramers $5f^2$ state does not develop an ordered dipole or quadrupolar moment, because both the z component and the transverse moment of the pseudovector $\langle \chi^\dagger \vec{\sigma} \chi \rangle = 0$ identically vanish. In the microscopic model, the quadrupolar moments vanish because of the d-wave form factor between the Γ_6 and Γ_7 channels (Supplementary Information). The absence of a charge quadrupole implies that there will be no lattice distortion associated with hastatic order. By contrast, hastatic order does induce a weak broken tetragonal symmetry in the spin channel. In the hidden-order state, the interchannel components of the hastatic t matrix, $\hat{\mathcal{V}}_6\hat{\mathcal{V}}_7^\dagger \propto \sigma_x + \sigma_y$, break tetragonal symmetry in the spin channel, resulting in a non-zero spin susceptibility within the conduction fluid

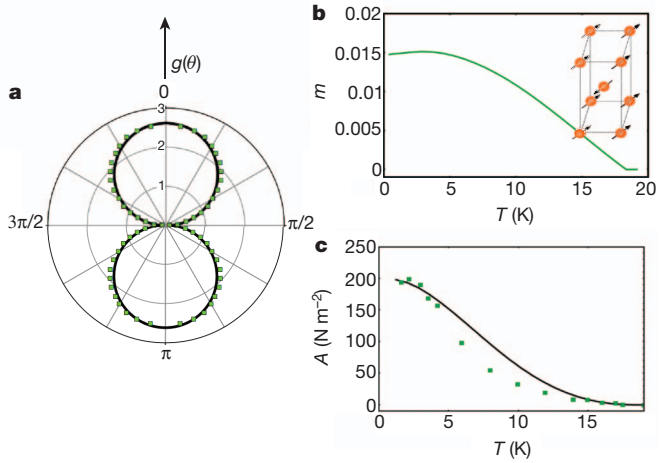

Figure 3 | Magnetic response of hastatic order. a, Polar plot of the calculated g-factor, $g(\theta)$, averaged over the Fermi surface, as a function of magnetic field angle, θ (see Supplementary Information for details), compared with results of ref. 20 (overlaid in green). **b**, As a consequence of the broken time-reversal symmetry, we predict a staggered conduction-electron moment that onsets at the HO transition with a linear, $T_{HO} - T$ temperature dependence (staggering pattern shown in inset). In the plot, the moment is expressed in Bohr magnetons per formula unit. The magnitude of this moment is governed by $T_K/D \approx 0.01\mu_B/U$, and its orientation is fixed by the way the uniform magnetic susceptibility breaks tetragonal symmetry. **c**, We calculated the tetragonal symmetry breaking component of the uniform susceptibility, $\chi_{xy}(T)$. To compare our results with those of ref. 18 (overlaid in green), we plotted the twofold oscillation amplitude of the magnetic torque, A (black), where $A\cos(2\phi) \equiv \tau_{2\phi}/V = -(\mu_0 H^2/V)\cos(2\phi)\chi_{xy}(T)$. This amplitude is proportional to $(T_{HO} - T)^2$ just below the hidden-order transition. For details of our calculation, including parameter choices, see Supplementary Information.

$$\chi_{xy} = -(g\mu_B)^2 \mathrm{Tr}\sigma_x \mathcal{G}^c(k,k+Q)\sigma_y \mathcal{G}^c(k+Q,k)$$
$$\propto \left(\mathrm{Tr}\hat{\mathcal{V}}_6\hat{\mathcal{V}}_7^\dagger\right)^2$$

of a magnitude of order $(T_K/D)^2$, which onsets at the hidden-order temperature as $|\Psi|^4 \approx (T_{HO} - T)^2$ as shown in Fig. 3c.

Hastatic order also manifests itself as an anisotropic hybridization gap, which vanishes along lines in momentum space, giving rise to a V-shaped density of states due to the partial gapping of the Fermi surface, as shown in Fig. 4, which will be smeared out by disorder in the real material. The anisotropy of the hybridization also breaks tetragonal symmetry, giving rise to a energy-dependent nematicity, $\eta(E)$, that peaks over a narrow energy window around the Kondo resonance. Some of this nematicity is present at the Fermi surface, accounting for the splitting seen in quantum oscillation frequencies[22] and cyclotron resonance experiments[47]. An ideal way to verify this prediction is to use scanning tunnelling spectroscopy, where the measured differential conductivity, $dI/dV \propto A(eV,x)$ is proportional to the local density of states $A(eV,x)$ at position x on the surface. A measure of the broken tetragonal symmetry is provided by the 'nematicity'

$$\eta(V) = \frac{\overline{(dI/dV)(x,y)\ \mathrm{sgn}(xy)}}{\left(\overline{(dI/dV)^2} - \left(\overline{dI/dV}\right)^2\right)^{1/2}}$$

Here x and y are the coordinates relative to the centre of the unit cell and the overbar denotes an average over the unit cell. The resonant scattering of the hastatic order causes this quantity to vary rapidly as a function of voltage, over an energy range of order the Kondo temperature T_K. Figure 4 shows the variation of the nematicity, calculated within our model of hastatic order. The nematicity is found to peak at the Kondo resonance, at a value of approximately 50%.

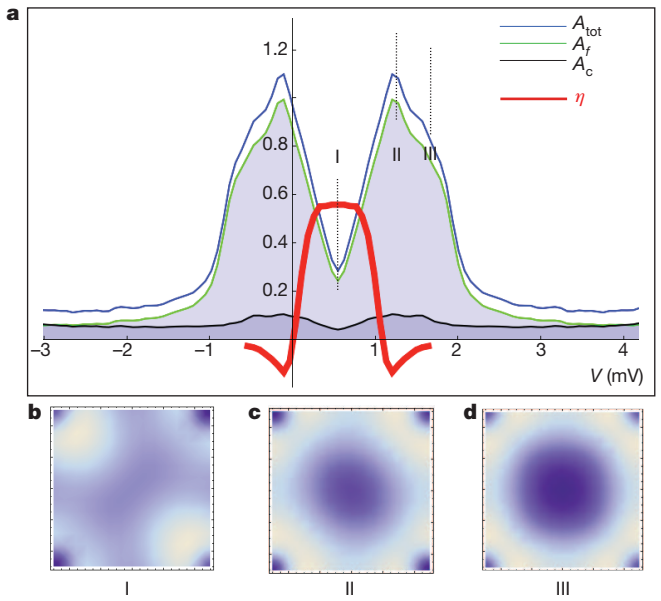

Figure 4 | Density of states and resonant nematicity predicted by theory. **a**, Density of states (arbitrary units) as a function of energy predicted by model calculation (blue line), showing *f*-electron and conduction-electron components. Red line, voltage dependence of nematicity, $\eta(V)$, in model calculation of scanning tunnelling spectrum. **b**–**d**, Spatial dependence of density of states for selected bias voltages in model calculation of scanning tunnelling spectrum, showing the resonant character of the nematicity. Voltages I, II and III are located at the center, the maximum and the shoulder of the density of states, respectively.

Beyond mean-field theory

So far we have focused on the mean-field consequences of hastatic order. The recently observed softening of the commensurate longitudinal spin fluctuations at T_{HO} (ref. 48) suggests that hastatic order 'melts' via phase fluctuations (the hastatic-order parameter vanishes but correlations remain). Although the hybridization spinor itself, $\langle \Psi \rangle$, can become non-zero only below the phase transition at T_{HO}, we expect that its amplitude, $\langle \Psi^\dagger \Psi \rangle$, will have a non-zero value to higher temperatures. Because $\langle \Psi^\dagger \vec{\sigma} \Psi \rangle$ remains zero above T_{HO}, only the non-symmetry-breaking (uniform, intrachannel) components of the hybridization can develop: $\hat{\mathcal{V}}_6 \hat{\mathcal{V}}_6^\dagger$ and $\hat{\mathcal{V}}_7 \hat{\mathcal{V}}_7^\dagger$ will emerge via a crossover at a higher temperature, T^*, to create an incoherent Fermi liquid, consistent with the heavy mass inferred from thermodynamic and optical measurements[1,17] and the development of Fano signatures in both scanning and point-contact tunnelling spectroscopy[14–16]. The symmetry-breaking, interchannel components, $\hat{\mathcal{V}}_6 \sigma_1 \hat{\mathcal{V}}_7^\dagger$, will always develop precisely at the hidden-order transition. Another aspect of experiments that is not covered by our mean-field description is the observation of gapped, low-energy incommensurate fluctuations around a Q-vector $Q^* = (1 \pm 0.4, 0, 0)$ in the hidden-order phase[33,35,48,49], which seems to be a sign of an unfulfilled predisposition towards an incommensurate phase, probably driven by partial Fermi surface nesting. These effects lie beyond a mean-field description, but would emerge from the Gaussian fluctuations about the mean-field theory.

Although we have discussed hastatic order in the context of URu_2Si_2, it should be a more widespread phenomenon associated with hybridization in any *f*-electron material whose unfilled *f* shell contains a geometrically stabilized non-Kramers doublet. As such, we expect realizations of hastatic order in other 5*f* uranium and 4*f* praseodymium intermetallic compounds.

Received 17 July; accepted 27 November 2012.

1. Palstra, T. T. M. *et al.* Superconducting and magnetic transitions in the heavy-fermion system URu_2Si_2. *Phys. Rev. Lett.* **55,** 2727–2730 (1985).
2. Schlabitz, W. *et al.* Superconductivity and magnetic order in a strongly interacting Fermi system: URu_2Si_2. *Z. Phys. B* **62,** 171–177 (1986).
3. Mydosh, J. A. & Oppeneer, P. M. Hidden order, superconductivity and magnetism – the unsolved case of URu_2Si_2. *Rev. Mod. Phys.* **83,** 1301–1322 (2011).
4. Amitsuka, H. & Sakakibara, T. Single uranium-site properties of the dilute heavy electron system $U_xTh_{1-x}Ru_2Si_2$ ($x \leq 0.07$). *J. Phys. Soc. Jpn* **63,** 736–747 (1994).
5. Haule, K. & Kotliar, G. Arrested Kondo effect and hidden order in URu_2Si_2. *Nature Phys.* **5,** 796–799 (2009).
6. Santini, P. & Amoretti, G. Crystal field model of the magnetic properties of URu_2Si_2. *Phys. Rev. Lett.* **73,** 1027–1030 (1994).
7. Varma, C. M. & Zhu, L. Helicity order: hidden order parameter in URu_2Si_2. *Phys. Rev. Lett.* **96,** 036405–036408 (2006).
8. Pépin, C., Norman, M. R., Burdin, S. & Ferraz, A. Modulated spin liquid: a new paradigm for URu_2Si_2. *Phys. Rev. Lett.* **106,** 106601–106604 (2011).
9. Yuan, T., Figgins, J. & Morr, D. K. Hidden order transition in URu_2Si_2: evidence for the emergence of a coherent Anderson lattice from scanning tunneling spectroscopy. *Phys. Rev. B* **86,** 035129–035134 (2012).
10. Dubi, Y. & Balatsky, A. V. Hybridization wave as the 'hidden order' in URu_2Si_2. *Phys. Rev. Lett.* **106,** 086401–086404 (2011).
11. Fujimoto, S. Spin nematic state as a candidate of the hidden order phase of URu_2Si_2. *Phys. Rev. Lett.* **106,** 196407–196410 (2011).
12. Ikeda, H. *et al.* Emergent rank-5 'nematic' order in URu_2Si_2. *Nature Phys.* **8,** 528–533 (2012).
13. Santander-Syro, A. F. *et al.* Fermi-surface instability at the 'hidden order' transition of URu_2Si_2. *Nature Phys.* **5,** 637–641 (2009).
14. Schmidt, A. R. *et al.* Imaging the Fano lattice to 'hidden order' transition in URu_2Si_2. *Nature* **465,** 570–576 (2010).
15. Aynajian, P. *et al.* Visualizing the formation of the Kondo lattice and the hidden order in URu_2Si_2. *Proc. Natl Acad. Sci. USA* **107,** 10383–10388 (2010).
16. Park, W. K. *et al.* Fano resonance and hybridization gap in Kondo lattice URu_2Si_2. *Phys. Rev. Lett.* **108,** 246403 (2012).
17. Nagel, U. *et al.* Optical spectroscopy shows that the normal state of URu_2Si_2 is an anomalous Fermi liquid. *Proc. Natl Acad. Sci. USA* **109,** 19161–19165 (2012).
18. Okazaki, R. *et al.* Rotational symmetry breaking in the hidden order phase of URu_2Si_2. *Science* **331,** 439–442 (2011).
19. Hassinger, E. *et al.* Similarity of the Fermi surface in the hidden order state and in the antiferromagnetic state of URu_2Si_2. *Phys. Rev. Lett.* **105,** 216409–216412 (2010).
20. Altarawneh, M. M. *et al.* Sequential spin polarization of the Fermi surface pockets of URu_2Si_2 and its implications for the hidden order. *Phys. Rev. Lett.* **106,** 146403–146416 (2011).
21. Ramirez, A. P. *et al.* Nonlinear susceptibility as a probe of tensor spin order in URu_2Si_2. *Phys. Rev. Lett.* **68,** 2680–2683 (1992).
22. Ohkuni, H. *et al.* Fermi surface properties and de Haas-van Alphen oscillation in both the normal and superconducting mixed states of URu_2Si_2. *Philos. Mag. B* **79,** 1045–1077 (1999).
23. Brison, J. P. *et al.* Anisotropy of the upper critical field in URu_2Si_2 and FFLO state in antiferromagnetic superconductors. *Physica C* **250,** 128–138 (1995).
24. Altarawneh, M. M. *et al.* Superconducting pairs with extreme uniaxial anisotropy in URu_2Si_2. *Phys. Rev. Lett.* **108,** 066407–066410 (2012).
25. Goremychkin, E. A. *et al.* Magnetic correlations and the anisotropic Kondo effect in $Ce_{1-x}La_xAl_3$. *Phys. Rev. Lett.* **89,** 147201–147204 (2002).
26. Flint, R., Chandra, P. & Coleman, P. Basal-plane nonlinear susceptibility: a direct probe of the single-ion physics in URu_2Si_2. *Phys. Rev. B* **86,** 155155–155160 (2012).
27. Nieuwenhuys, G. J. Crystalline electric field effects in UPt_2Si_2 and URu_2Si_2. *Phys. Rev. B* **35,** 5260–5263 (1987).
28. Zołnierek, Z. & Troc, R. Magnetic properties of tetragonal uranium componds. I. The U_2N_2Z ternaries. *J. Magn. Magn. Mater.* **8,** 210–222 (1978).
29. Ohkawa, F. J. & Shimizu, H. Quadrupole and dipole orders in URu_2Si_2. *J. Phys. Condens. Matter* **11,** L519–L524 (1999).
30. Sakurai, J. J. *Modern Quantum Mechanics* rev. edn 266–282 (Addison-Wesley, 1994).
31. Amitsuka, H. *et al.* Pressure-temperature phase diagram of the heavy-electron superconductor URu_2Si_2. *J. Magn. Magn. Mater.* **310,** 214–220 (2007).
32. Jo, Y. J. *et al.* Field-induced Fermi surface reconstruction and adiabatic continuity between antiferromagnetism and the hidden-order state in URu_2Si_2. *Phys. Rev. Lett.* **98,** 166404 (2007).
33. Villaume, A. *et al.* Signature of hidden order in heavy fermion superconductor URu_2Si_2: resonance at the wave vector $Q_0 = (1, 0, 0)$. *Phys. Rev. B* **78,** 012504 (2008).
34. Haule, K. & Kotliar, G. Complex Landau-Ginzburg theory of the hidden order in URu_2Si_2. *Europhys. Lett.* **89,** 57006 (2010).
35. Broholm, C. *et al.* Magnetic excitations in the heavy-fermion superconductor URu_2Si_2. *Phys. Rev. B* **43,** 12809–12822 (1991).
36. Miyako, Y. *et al.* Magnetic properties of $U(Ru_{1-x}Rh_x)_2Si_2$ single crystals ($0 \leq x \leq 1$). *J. Appl. Phys.* **70,** 5791 (1991).
37. Cox, D. L. & Jarrell, M. The two-channel Kondo route to non-Fermi liquids. *J. Phys. Condens. Matter* **8,** 9825–9853 (1996).
38. Cox, D. L. & Zawadowski, A. *Exotic Kondo Effects in Metals* (Taylor & Francis, 2002).
39. Coleman, P. A new approach to the mixed valence problem. *Phys. Rev. B* **29,** 3035–3044 (1984).
40. Coleman, P., Tsvelik, A. M., Andrei, N. & Kee, H. Y. Co-operative Kondo effect in the two-channel Kondo lattice. *Phys. Rev. B* **60,** 3608–3628 (1999).
41. Hoshino, S., Otsuki, J. & Kuramoto, Y. Diagonal composite order in a two-channel Kondo lattice. *Phys. Rev. Lett.* **107,** 247202–247205 (2011).

42. Bolech, C. & Andrei, N. Solution of the two-channel Anderson impurity model: implications for the heavy fermion UBe_{13}. *Phys. Rev. Lett.* **88,** 237206–237209 (2002).
43. Coleman, P., Marston, J. B. & Schofield, A. J. Transport anomalies in a simplified model for a heavy-electron quantum critical point. *Phys. Rev. B* **72,** 245111 (2003).
44. Anderson, P. W. Localized magnetic states in metals. *Phys. Rev.* **124,** 41–53 (1961).
45. Amitsuka, H. *et al.* Inhomogeneous magnetism in URu_2Si_2 studied by muon spin relaxation under high pressure. *Physica B* **326,** 418–421 (2003).
46. Bernal, O. O. *et al.* Ambient pressure ^{99}Ru NMR in URu_2Si_2: internal field anisotropy. *J. Magn. Magn. Mater.* **272–276,** E59–E60 (2004).
47. Tonegawa, S. *et al.* Cyclotron resonance in the hidden-order phase of URu_2Si_2. *Phys. Rev. Lett.* **109,** 036501 (2012).
48. Niklowitz, P. G. *et al.* Role of commensurate and incommensurate low-energy excitations in the paramagnetic to hidden-order transition of URu_2Si_2. Preprint at http://arxiv.org/abs/1110.5599 (2011).
49. Wiebe, C. R. *et al.* Gapped itinerant spin excitations account for missing entropy in the hidden order state of URu_2Si_2. *Nature Phys.* **3,** 96–99 (2007).

Supplementary Information is available in the online version of the paper.

Acknowledgements An early version of this work was begun in collaboration with P. Fazekas, since deceased. We thank N. Andrei, S. Burdin, B. Coleman, L. Greene, N. Harrison, K. Haule, G. Kotliar, P. Lee, G. Luke, Y. Matsuda, J. Mydosh, P. Niklowitz, C. Pépin, T. Senthil, A. Toth and T. Timusk for discussions. We acknowledge funding from the Simons Foundation (R.F.), the US National Science Foundation grant DMR 0907179 (R.F., P. Coleman), the US National Science Foundation I2CAM International Materials Institute Award Grant DMR-0844115 (R.F., P. Coleman) and the US National Science Foundation grant 1066293 (all authors) while at the Aspen Center for Physics. We are grateful for the hospitality of the Aspen Center for Physics.

Author Contributions All authors contributed equally in the discussions and development of the hastatic-order concept, the experimental consequences and its mean-field description pertinent to URu_2Si_2. R.F. and P. Coleman carried out the detailed numerical calculations of the microscopic model. All authors contributed towards the writing of the paper and Supplementary Information.

Author Information Reprints and permissions information is available at www.nature.com/reprints. The authors declare no competing financial interests. Readers are welcome to comment on the online version of the paper. Correspondence and requests for materials should be addressed to P. Coleman. (coleman@physics.rutgers.edu).